Constrained tricritical Blume-Capel model in three dimensions

Youjin Deng[1] and Henk W. J. Blöte[1,2]
[1]*Laboratory for Material Science, Delft University of Technology, Rotterdanseweg 137, 2628 AL Delft, The Netherlands*
[2]*Lorentz Institute, Leiden University, P. O. Box 9506, 2300 RA Leiden, The Netherlands*
(Received 14 June 2004; published 21 October 2004)

Using the Wolff and geometric cluster Monte Carlo methods, we investigate the tricritical Blume-Capel model in three dimensions. Since these simulations conserve the number of vacancies and thus effectively introduce a constraint, we generalize the Fisher renormalization for constrained critical behavior to tricritical systems. We observe that, indeed, the tricritical behavior is significantly modified under this constraint. For instance, at tricriticality, the specific heat has only a finite cusp and the Binder ratio assumes a different value from that in unconstrained systems. Since 3 is the upper tricritical dimensionality of Ising systems, we expect that the mean-field theory correctly predicts a number of universal parameters in three dimensions. Therefore, we calculate the partition sum of the mean-field tricritical Blume-Capel model, and accordingly obtain the exact value of the Binder ratio. Under the constraint, we show that this mean-field *tricritical* system reduces to the mean-field *critical* Ising model. However, our three-dimensional data do not agree with this mean-field prediction. Instead, they are successfully explained by the generalized Fisher renormalization mechanism.

DOI: 10.1103/PhysRevE.70.046111 PACS number(s): 05.50.+q, 64.60.Cn, 64.60.Fr, 75.10.Hk

I. INTRODUCTION

In the development of the theory of critical phenomena and phase transitions, a spin-1 Ising model known as the Blume-Capel (BC) model has played an important role. This model was originally introduced by Blume and Capel [1,2], and the reduced Hamiltonian reads

$$\mathcal{H}/k_{\mathrm{B}}T = -K\sum_{\langle ij\rangle} s_i s_j + D\sum_k s_k^2 \quad (s_i = \pm 1, 0), \tag{1}$$

where the sum $\langle\ \rangle$ is over all nearest-neighbor pairs of lattice sites. The spins assume values ± 1 and 0, and those in state 0 are referred to as vacancies. The abundance of vacancies is governed by the chemical potential D, which is also termed the crystal field parameter. The phase diagram is sketched in Fig. 1. For $D \to -\infty$, the vacancies are excluded, and the model (1) reduces to Onsager's spin-$\frac{1}{2}$ model [3]. The critical couping $K_c(D)$ is an increasing function of D. For sufficiently large chemical potential, the transition then becomes first order, separating the vacancy-dominated phase from those dominated by plus (+1) or minus (−1) spins. At the joint point, these three coexisting phases *simultaneously* become identical, and this point is then called [4] the tricritical point, denoted as (K_t, D_t) in Fig. 1.

In two dimensions, the nature of critical singularities of the BC model is now well established. For instance, as early as in 1942, the exact expression of the free energy was obtained by Onsager [3,5] for the spin-$\frac{1}{2}$ model. The universal thermal and magnetic exponents are $y_t = 1$ and $y_h = 15/8$, respectively. At the tricritical point (K_t, D_t), exact values of the universal exponents follow from Baxter's exact results for the hard-square lattice gas [6,7], in the same universality class as the tricritical Blume-Capel model; further, these exponents can be calculated from the Coulomb gas theory [8,9] and are also included in predictions of the conformal field theory [10,11]. The leading and subleading thermal exponents at tricriticality are [6–12] $y_{t1} = 9/5$ and $y_{t2} = 4/5$, respectively, and the magnetic ones are $y_{h1} = 77/40$ and $y_{h2} = 9/8$, respectively.

In three dimensions, exact results are absent for the BC model along the critical line $K_c(D)$, and investigations of critical behavior have to depend on approximations such as series and ϵ expansions, and Monte Carlo simulations [13–16]. However, the tricritical Ising model is somewhat special, in the sense that it is one of the rare cases in three dimensions that exact information is available about critical singularities [4]. This is possible because *3* is the upper tricritical dimensionality of Ising systems. As a consequence, critical exponents can be exactly obtained from renormalization calculations [17] of the Landau-Ginzburg-Wilson Hamiltonian. The thermal and magnetic tricritical exponents [4] are $y_{t1} = 2$ and $y_{t2} = 1$, and $y_{h1} = 5/2$ and $y_{h2} = 3/2$, respectively.

An experimental example of tricritical phenomena in three dimensions is the superfluid transition in ^{3}He-^{4}He mixtures [4], which is sketched in Fig. 2. The transition at the tricritical point is known as the λ transition. In fact, the order parameter in the ^{3}He-^{4}He mixtures is a vector of two components, so that the superfluid transition should in principle

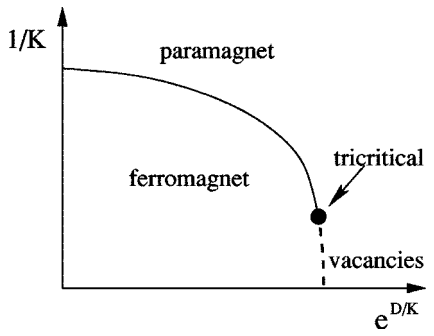

FIG. 1. Sketch of the phase diagram of the BC model. The solid line represents the critical line, which separates the para- and ferromagnetic phases; and the first-order transition is shown as a dashed line. The two lines join at a tricritical point (black circle).

 ©2004 The American Physical Society

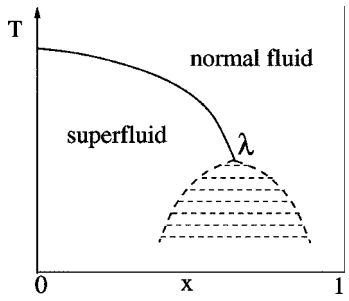

FIG. 2. The schematic phase diagram of a ^{3}He-^{4}He mixture in the plane of temperature T and mole fraction x of ^{3}He. The temperature can be understood as the inverse coupling constant $1/K$ in Eq. (1).

be described by the $O(2)$ model, the so-called XY model. Nevertheless, the renormalization calculations yield the same critical exponents for the $O(n)$ model with $n \geqslant 1$, apart from logarithmic corrections. Thus, in this sense, the BC model (1) is still qualitatively applicable [4] at the λ point. One would then simply expect that the tricritical specific heat C is *divergent*, with a critical index $\alpha = 2 - d/y_{t1} = 1/2$. However, this expectation does not agree with the existing experimental results: C was observed [18] to have only a *finite* cusp with $\alpha = -0.9(1)$ at the λ point.

This lack of agreement is the result of an important difference between the systems in the aforementioned theoretical and experimental contexts. This is reflected by the distinction between Figs. 1 and 2, of which the first deals with models in the space (K, D). In contrast, Fig. 2 uses the mole fraction x of ^{3}He as an independent parameter [18]. The fraction x plays a similar role as the vacancy density in Eq. (1). Therefore, a correct theoretical description of the λ transition in Fig. 2 should be based on a restricted partition sum with a conserved number of vacancies. In other words, an external constraint is imposed on the system (1). This constraint is of the "annealed" type [19] since vacancies are allowed to move freely over the lattice according to the Boltzmann distribution.

Constrained critical behavior has already been studied for decades. As earlier as 1965, Syozi [20] introduced a decorated Ising model on a d-dimensional lattice, which was shown [21] to be intimately connected with annealed systems. The Syozi model can be exactly transformed into the spin-$\frac{1}{2}$ model, and critical exponents of these two systems are related as

$$\alpha_s = -\alpha/(1-\alpha), \quad \beta_s = \beta/(1-\alpha), \quad \text{and} \quad \nu_s = \nu/(1-\alpha), \quad \ldots \tag{2}$$

where α and β are the standard critical indices for the specific heat C and the magnetization density m for the spin-$\frac{1}{2}$ model, respectively, and $\nu = 1/y_t$ is the inversion of the thermal exponent; those with the subscript "s" are for the Syozi model. It can be shown that the hyperscaling relations still hold among the critical indices α_s, β_s, etc. In three dimensions, the spin-$\frac{1}{2}$ model has $1 > \alpha > 0$, so that the specific heat C of the Syozi model does not diverge at criticality. In two dimensions, C of the spin-$\frac{1}{2}$ model is divergent in a logarithmic scale since $\alpha = 0$. For this marginal case, C of the Syozi model reaches a finite cusp, also of a logarithmic nature. Later, this was discussed in a more general context by Essam and Garelick [22] and by Fisher [23]. It was pointed out that relations (2) are not specific to the Syozi model, but are more generally satisfied by equilibrium models with a divergent specific heat ($\alpha > 0$). Since then, the so-called Fisher renormalization of constrained critical systems has gained considerable acceptance [24–27].

A description of constrained *tricritical* behavior was formulated by Imry and his co-workers [28] in the context of the renormalization group (RG) technique. Using the ϵ expansion and a generalized Landau-Ginzburg-Wilson Hamiltonian, they found four distinct fixed points: the tricritical Ising (TI), critical Ising (CI), *renormalized* tricritical Ising (RTI), and *renormalized* critical Ising (RCI) fixed points. Renormalization flows deviating from TI can move into the fixed point CI or RTI, and those from CI can end at the RCI point. The critical exponents at these fixed points are related as $\alpha_{RCI} = -\alpha_{CI}/(1-\alpha_{CI})$ and $\alpha_{RTI} = -\alpha_{TI}/(1-\alpha_{TI})$, in agreement with Eq. (2). For the spatial dimensionality $d \geqslant 3$, points TI and RTI correspond to Gaussian and spherical fixed points, respectively. Thus, one has the critical indices $\alpha_{TI} = 1/2$ and $\alpha_{RTI} = -\alpha_{TI}/(1-\alpha_{TI}) = -1$ in three dimensions. If one assumes that constrained behavior of an annealed tricritical system is governed by the fixed point RTI, the theoretical prediction $\alpha_{RTI} = -1$ is then in good agreement with the experimental observation [18] $\alpha = -0.9(1)$.

At the upper critical dimensionality, the mean-field theory is generally believed to correctly describe some universal aspects of phase transitions. Indeed, for the tricritical BC model in three dimensions, a number of universal quantities, including the thermal and magnetic exponents y_{t1} and y_{h1}, can be exactly calculated [4] from a mean-field (MF) analysis. In the present paper, we also perform some exact calculations for the MF BC model. Under the constraint that the total number of vacancies is fixed, we show that the *tricritical* MF BC model reduces to the *critical* MF Ising model. However, this MF result is not what one would expect for the tricritical BC model in three dimensions, since the constraint should not change the universality class. Thus, the present paper also takes another approach: following the basic ideas in Ref. [23], we generalize the Fisher renormalization mechanism for constrained *critical* behavior to tricritical systems. In particular, we derive finite-size scaling results based on this generalized mechanism.

In addition to these theoretical analyses, we perform a Monte Carlo study of the constrained three-dimensional (3D) BC model. For systems with a conserved number of vacancies, efficient simulations have become possible only after the introduction of the geometric cluster method [29–31]. This algorithm was developed on the basis of spatial symmetries, such as Hamiltonian invariance under spatial inversions and rotations. It moves groups of magnetic spins and vacancies over the lattice in accordance with Boltzmann distribution, while the global magnetization and vacancy densities are conserved. Then, the aforementioned constraint can be realized by a combination of the geometric method and

the Wolff algorithm [32], which acts only on nonzero spins and thus allows magnetization fluctuations.

The outline of the remaining part of this paper is as follows. Section II presents exact calculations of the tricritical MF BC model, and the Fisher renormalization mechanism is generalized to constrained tricritical systems in Sec. III. Section IV presents our Monte Carlo results for the 3D BC model, and a short discussion is given in Sec. V.

II. MEAN-FIELD BLUME-CAPEL MODEL

In this section, we perform an asymptotic analysis of the finite mean-field BC model. On this basis, we hope to obtain some exact results for universal parameters describing constrained behavior of the tricritical BC model in three dimensions.

The mean-field version of a finite BC model (1) is expressed by the Hamiltonian

$$\mathcal{H}/k_{\mathrm{B}}T = -\frac{K}{N}\sum_{i=1}^{N}\sum_{j=i+1}^{N} s_i s_j + D\sum_{k} s_k^2 \ (s_i = \pm 1, 0), \qquad (3)$$

where N is the total number of spins, and each spin is interacting with each other spin. Then, the local Hamiltonian of the ith spin, i.e., the terms in Eq. (3) involving that spin, reads

$$\mathcal{H}_i/k_{\mathrm{B}}T = -Ks_i m + Ds_i^2 + \frac{K}{N}s_i^2 \text{ with } mN = \sum_{i=1}^{N} s_i, \qquad (4)$$

where m is the global magnetization density. The last term in Eq. (4) vanishes as $1/N$, and will be neglected. The tricritical point [4] of this MF system can be calculated as follows. According to the Boltzmann distribution, Eq. (4) determines the statistical probability w of the local spin s_i as

$$w(s_i = 1) = \frac{1}{z}e^{Km}, \quad w(s_i = 0) = \frac{1}{z}e^{D},$$
$$\text{and } w(s_i = -1) = \frac{1}{z}e^{-Km}, \qquad (5)$$

with a normalization factor $z = e^{Km} + e^{D} + e^{-Km}$. Thus, the local magnetization $\langle s_i \rangle$ and the global one m are related as

$$\langle s_i \rangle = 2\sinh(Km)/[\exp(D) + 2\cosh(Km)]. \qquad (6)$$

At tricriticality, the stability criterion requires that $m = 0$, $\partial\langle s_i\rangle/\partial m = 1$, and $\partial^3\langle s_i\rangle/\partial m^3 = 0$. From Eq. (6), solution of these requirements yields the tricritical point as $K_t = 3$ and $D_t = 2\ln 2$, and the corresponding vacancy density as $\rho_v = \rho_{vt} = 2/3$.

A. Unconstrained systems

The Hamiltonian (3) depends only the numbers of down spins and vacancies, which are denoted as N_d and N_v, respectively. Expression of the partition sum Z in these variables leads to

$$Z = \sum_{N_d=0}^{N}\sum_{N_v=0}^{N-N_d} c(N_d, N_v)\exp\left[\frac{K}{2}N\left(\frac{N - N_v - 2N_d}{N}\right)^2 - \left(D + \frac{K}{2N}\right)(N - N_v)\right], \qquad (7)$$

where the combinatorial factor $c(N_d, N_v)$ counts the total number of configurations with N_d minus spins and N_v vacancies

$$C(N_d, N_v) = \frac{N!}{N_d!\, N_v!\, (N - N_d - N_v)!}. \qquad (8)$$

After the substitution of the magnetization density $m = (N - N_v - 2N_d)/N$ and the vacancy density $\rho_v = N_v/N$ in Eqs. (7) and (8), one has

$$Z = 2N^2\int_0^1 dm\int_0^1 d\rho_v\, c(m, \rho_v)\exp\left(\frac{K}{2}Nm^2 - DN(1 - \rho_v)\right) \times[1 + O(1/N)], \qquad (9)$$

where we have replaced the sums in Eq. (7) by integrals over the magnetization and vacancy density m and ρ_v, and neglected correction terms of order $1/N$. Substitution of the tricritical values of K and D, application of the Stirling's formula $\ln(N!) = (N + \frac{1}{2})\ln N - N$, and Taylor expansion of $\ln c(m, \rho_v)$ yield

$$\ln c(m, \rho_v) = -\frac{9}{4}N(\delta\rho_v + m^2)^2 - \frac{81}{4}N\delta\rho_v m^4 - \frac{27}{2}N(\delta\rho_v)^2 m^2 - \frac{9}{8}N(\delta\rho_v)^3 - \frac{81}{10}Nm^6 + NO[m^{8-2k}(\delta\rho_v)^k] + \cdots \quad (k = 0, 1, 2, 3, 4) \qquad (10)$$

where $\delta\rho_v = \rho_v - \rho_{vt}$ represents fluctuations of the vacancies. On this basis, the partition sum (9) can be written as

$$Z = fN^2\int_0^\infty dm\, e^{-(81/10)Nm^6}[1 + NO(m^8)]\int_{-\infty}^{\infty} d\tilde{\rho}\, e^{-(9/4)N\tilde{\rho}^2} \times\left(1 + \tfrac{63}{8}Nm^6 + NO(m^8)\right)$$
$$= f'N^2\int_0^\infty dm\, e^{-(9/40)Nm^6}\int_{-\infty}^{\infty} d\tilde{\rho}\, e^{-(9/4)N\tilde{\rho}^2} \times[1 + O(1/N)], \qquad (11)$$

where f and f' are constants and we have introduced a new variable $\tilde{\rho} = \delta\rho_v + m^2$. The integration boundaries have been extended to infinity, and this can be shown [33,34] to introduce only an error decaying exponentially with N. Equation (11) indicates that the tricritical fluctuations of the MF BC model (3) consist of two parts: Gaussian (normal) fluctuations of a combined variable $\tilde{\rho}$ and those of the magnetization described by a weight $\exp(-9Nm^6/40)$. The absence of m^2 and m^4 in Eq. (11) is an essential characteristic of the ϕ^6 theory and the mean-field description of tricritical phenomena. For later convenience, we rewrite Eq. (11) in the variables $x_m = 9Nm^6/40$ and $x_v = 9N\tilde{\rho}^2/4$ as

$$Z = B(N) \int_0^\infty dx_m\, x_m^{-5/6}\, e^{-x_m} \int_0^\infty dx_v\, x_v^{-1/2}\, e^{-x_v} [1 + O(1/\sqrt[3]{N})], \tag{12}$$

where $B(N)$ is a function of N. Then, substitution of the Γ function $\Gamma(z) = \int_0^\infty u^{z-1} e^{-z} dz$ yields the partition sum (11) as

$$Z = B(N) \Gamma\left(\tfrac{1}{6}\right) \Gamma\left(\tfrac{1}{2}\right). \tag{13}$$

In the study critical phenomena, several universal ratios of finite-size scaling amplitudes, closely related to the quantity originally introduced by Binder [35], play an important role. Particularly, these dimensionless ratios are very useful in Monte Carlo determinations of critical points. Here, we consider two such ratios, which are defined on the basis of fluctuations of the magnetization m and vacancy density ρ_v as

$$Q_m = \frac{\langle m^2 \rangle^2}{\langle m^4 \rangle} \text{ and } Q_v = \frac{\langle (\delta\rho_v)^2 \rangle^2}{\langle (\delta\rho_v)^4 \rangle}, \tag{14}$$

with $\delta\rho_v = \rho_v - \rho_{vt}$, as mentioned earlier.

From the probability distribution implied by the partition sum (12), the expectation values of the moments of the magnetization density m are then obtained as

$$\langle m^2 \rangle = \frac{B(N)}{Z} \int_0^\infty dx_m\, m^2 x_m^{-5/6} e^{-x_m} \int_0^\infty dx_v\, x_v^{-1/2}\, e^{-x_v}$$

$$= \left(\frac{40}{9N}\right)^{1/3} \frac{\Gamma\left(\frac{1}{2}\right)}{\Gamma\left(\frac{1}{6}\right)} + O(N^{-2/3}),$$

$$\langle m^4 \rangle = \left(\frac{40}{9N}\right)^{2/3} \frac{\Gamma\left(\frac{5}{6}\right)}{\Gamma\left(\frac{1}{6}\right)} + O(N^{-1}),$$

$$\langle m^6 \rangle = \left(\frac{40}{9N}\right) \frac{\Gamma\left(\frac{7}{6}\right)}{\Gamma\left(\frac{1}{6}\right)} + O(N^{-4/3}),$$

and

$$\langle m^8 \rangle = \left(\frac{40}{9N}\right)^{4/3} \frac{\Gamma\left(\frac{3}{2}\right)}{\Gamma\left(\frac{1}{6}\right)} + O(N^{-5/3}). \tag{15}$$

Therefore, the dimensionless ratio Q_m is

$$Q_m = \Gamma^2\left(\tfrac{1}{2}\right) / \Gamma\left(\tfrac{1}{6}\right) \Gamma\left(\tfrac{5}{6}\right) + O(N^{-1/3}) = \tfrac{1}{2} + O(N^{-1/3}), \tag{16}$$

where we have used the formula $\Gamma\left(\frac{1}{2}+z\right)\Gamma\left(\frac{1}{2}-z\right) = \pi/\cos(\pi z)$, so that $\Gamma^2\left(\frac{1}{2}\right) = \pi$ and $\Gamma\left(\frac{1}{6}\right)\Gamma\left(\frac{5}{6}\right) = 2\pi$.

The exact value of Q_v can be obtained as follows. From the definition $\tilde{\rho} = \delta\rho_v + m^2$, one has

$$\langle \delta\rho_v \rangle = \langle \tilde{\rho} \rangle - \langle m^2 \rangle,$$

$$\langle (\delta\rho_v)^2 \rangle = \langle \tilde{\rho}^2 \rangle - 2\langle \tilde{\rho} \rangle \langle m^2 \rangle + \langle m^4 \rangle,$$

and

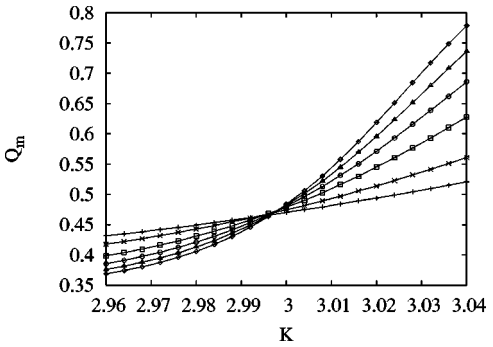

FIG. 3. The Binder ratio Q_m of the MF BC model at $D_t = 2 \ln 2$ for $2.96 \leqslant K \leqslant 3.04$. The data points are $N = 100$ (+), 200 ($\times$), 400 ($\square$), 600 ($\bigcirc$), 800 ($\triangle$), and 1000 ($\diamond$).

$$\langle (\delta\rho_v)^4 \rangle = \langle \tilde{\rho}^4 \rangle - 4\langle \tilde{\rho}^3 \rangle \langle m^2 \rangle + 6\langle \tilde{\rho}^2 \rangle \langle m^4 \rangle - 4\langle \tilde{\rho} \rangle \langle m^6 \rangle + \langle m^8 \rangle. \tag{17}$$

At the tricritical point, one has $\langle \delta\rho_v \rangle = 0$, so that $\langle \tilde{\rho} \rangle = \langle m^2 \rangle$. A detailed calculation then yields

$$Q_v^{-1} = \left(-3 + 6\frac{\langle m^4 \rangle}{\langle m^2 \rangle^2} - 4\frac{\langle m^6 \rangle}{\langle m^2 \rangle^3} + \frac{\langle m^8 \rangle}{\langle m^2 \rangle^4} \right) \Bigg/ \left(\frac{\langle m^4 \rangle}{\langle m^2 \rangle^2} - 1 \right)^2, \tag{18}$$

so that

$$Q_v^{-1} = 9 - \tfrac{1}{6} \left[\frac{\Gamma\left(\frac{1}{6}\right)}{\Gamma\left(\frac{1}{2}\right)} \right]^3 \simeq 3.8348, \tag{19}$$

and $Q_v = 0.2608\ldots$.

The aforementioned calculations implicitly yield the mean-field thermal and magnetic exponents. Equation (4) indicates that the mean-field quantity $\langle m^2 \rangle$ can be regarded as a type of energy density. From the definition of the magnetic susceptibility $\chi = N\langle m^2 \rangle$, one has then the scaling behavior at tricriticality $\langle m^2 \rangle \propto N^{\tilde{y}_t - 1} = N^{2\tilde{y}_h - 2}$. Here, we have introduced the mean-field critical exponents $\tilde{y}_t$ and $\tilde{y}_h$, which are related to the standard leading thermal and magnetic exponents in finite dimensions as $y_{t1} = d\tilde{y}_t$ and $y_{h1} = d\tilde{y}_h$ with $d \geqslant 3$, respectively. The above scaling formula gives the mean-field relation $\tilde{y}_t = 2\tilde{y}_h - 1$, which generally holds for mean-field systems. On this basis, Eq. (15) yields $\tilde{y}_t = 2/3$ and $\tilde{y}_h = 5/6$ for the tricritical MF BC model, so that one has $y_{t1} = 2$ and $y_{h1} = 5/2$ in three dimensions, in agreement with the existing RG results [4].

B. Monte Carlo simulations

The mean-field calculations in the above subsection rely on the limit $N \to \infty$, and thus we have performed numerical tests for finite N. Using the standard Metropolis method, which is adequate for this purpose, we simulated the unconstrained model (3) for $D = D_t = 2 \ln 2$ in the range $2.96 \leqslant K \leqslant 3.04$. The system sizes were taken as $N = 100$, 200, 400, 600, 800, and 1000. The MF result for the tricritical point is confirmed by the clear intersection of the Q_m versus K data, shown in Fig. 3 at $K = 3$. Then we simulated precisely at the

TABLE I. Monte Carlo data for ρ_v, Q_m, and Q_v for the MF BC model at the tricritical point $K_t=3$ and $D_t=2\ln 2$. The numbers in parentheses represent the error margins in the last decimal place.

N	10	20	40	60	100	200	300
ρ_v	0.53364(3)	0.54314(3)	0.55756(3)	0.56666(2)	0.57804(2)	0.59251(2)	0.60027(2)
Q_m	0.45159(5)	0.45815(6)	0.46352(6)	0.46644(6)	0.46992(6)	0.47449(7)	0.47694(8)
Q_v	0.40132(5)	0.36988(6)	0.34546(7)	0.33388(7)	0.32129(8)	0.30746(8)	0.30099(9)
N	400	600	1000	2000	4000	8000	16000
ρ_v	0.60541(2)	0.61211(2)	0.61970(1)	0.62852(1)	0.63587(1)	0.64183(1)	0.64678(2)
Q_m	0.47853(8)	0.4806(1)	0.4831(1)	0.4862(1)	0.4886(1)	0.4910(2)	0.4922(2)
Q_v	0.29683(9)	0.2918(1)	0.2865(1)	0.2807(1)	0.2763(1)	0.2732(2)	0.2700(2)

tricritical point (K_t, D_t), with system sizes $10 \leqslant N \leqslant 16\,000$. The sampled quantities include the magnetic susceptibility $\chi = N\langle m^2\rangle$, the vacancy density ρ_v, and the Binder ratios Q_m and Q_v. Here, the quantity Q_v is defined by Eq. (14), but $\delta\rho_v = \rho_v - \rho_{vt}$ is replaced by $\delta\rho_v = \rho_v - \langle\rho_v\rangle$ for finite systems. The latter definition of Q_v is more natural in the sense that, for finite-dimensional systems, the exact value of ρ_{vt} is generally unknown. Further, at tricriticality, since the quantity $\langle\rho_v\rangle$ approaches ρ_{vt} as $N\to\infty$, these two definitions do not have qualitative difference. The data for ρ_v, Q_m, and Q_v are shown in Table I. According to the least-squares criterion, we fitted the Monte Carlo data by

$$\chi(N) = \chi_0 + N^{2\tilde{y}_h-1}(x_0 + x_1 N^{\tilde{y}_i} + x_2 N^{2\tilde{y}_i} + x_3 N^{3\tilde{y}_i}),$$

$$\rho_v(N) = \rho_{vt} + N^{\tilde{y}_t-1}(p_0 + p_1 N^{\tilde{y}_i} + p_2 N^{2\tilde{y}_i} + p_3 N^{3\tilde{y}_i}),$$

$$Q_m(N) = Q_{mt} + q_{m1} N^{\tilde{y}_i} + q_{m2} N^{2\tilde{y}_i} + q_{m3} N^{3\tilde{y}_i},$$

and

$$Q_v(N) = Q_{vt} + q_{v1} N^{\tilde{y}_i} + q_{v2} N^{2\tilde{y}_i} + q_{v3} N^{3\tilde{y}_i}. \tag{20}$$

The terms with the exponent $\tilde{y}_i$ account for finite-size corrections, with $\tilde{y}_i = -1/3$, as indicated from Eq. (16). Results are given in Table II, where the estimation of $\tilde{y}_i$ was obtained from the fit of Q_m with Q_{mt} fixed at $1/2$. The theoretical predictions and the numerical determinations are in fine agreement. For clarity, the data for Q_v is shown in Fig. 4 as $Q_v - q_{v2}N^{-2/3}$ versus $N^{-1/3}$, with q_{v2} taken from the fit.

These exact results are not only theoretically interesting, but also practically useful. For instance, the exact values of Q_{mt} and Q_{vt} are very helpful in a Monte Carlo determination [36] of the tricritical point of BC models in three dimensions.

C. Constrained systems

For the MF BC model (3) with a conserved number of vacancies, the reduced partition sum is obtained from Eq. (9) by excluding the integration over vacancy fluctuations:

$$Z' = N^2 \int dm\ \delta_{\rho_v,2/3} c(m,\rho_v) \exp\left(\frac{K}{2} N m^2 - DN(1-\rho_v)\right) \times [1 + O(1/N)]. \tag{21}$$

It can be shown that, at the tricritical point (K_t, D_t), Eq. (21) reduces to

$$Z' = N^2 \int dm\ e^{-(9/4)Nm^4}[1 + O(Nm^6)], \tag{22}$$

which characterizes the *critical* mean-field Ising model [17,33,34].

The reduction to the *critical* MF Ising model can be further understood as follows. In mean-field systems, each spin interacts with each other spin. Only the number of vacancies, not their positions, matters. One can then rearrange the labels of the Ising spins and those of the vacancies, such that all Ising spins are counted from 1 to $N/3$ and vacancies from $N/3+1$ to N. Then, the constrained Hamiltonian reads

$$\mathcal{H}/k_BT = -\frac{K'}{N'}\sum_{i=1}^{N'} + 2DN' \sum_{j=i+1}^{N'} s_i s_j (s_i = \pm 1), \tag{23}$$

where the sum is now only over $N' = N/3$ Ising spins, and $K' = K/3$ is the coupling constant in Eq. (23). For $K = K_t = 3$, Eq. (23) describes a MF critical Ising model with N' spins, and the critical point is at $K' = K'_c = 1$. In this case, the Binder ratio Q_m assumes $4\Gamma^2\left(\frac{3}{4}\right)/\Gamma^2\left(\frac{1}{4}\right) = 0.4569\ldots$ [(33) and (34)].

TABLE II. Results of a least-squares analysis of the Monte Carlo data for the MF BC model at the tricritical point $K_t=3$ and $D_t=2\ln 2$. The numbers in parentheses represent the error margins in the last decimal place.

	$\tilde{y}_h$	$\tilde{y}_t$	$\tilde{y}_i$	ρ_{vt}	Q_{mt}	Q_{vt}
Theory	5/6	2/3	−1/3	2/3	1/2	0.2608…
Fit	0.833(2)	0.667(2)	−0.332(1)	0.66664(6)	0.4998(3)	0.2609(3)

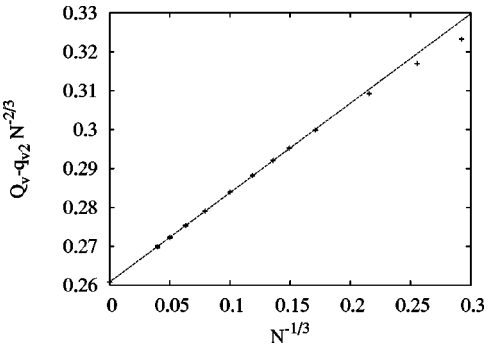

FIG. 4. The Binder ratio Q_v of the MF BC model at tricriticality. The data $Q_v - q_{v2} N^{-2/3}$ are shown vs $N^{-1/3}$, where $q_{v2} = 0.26(2)$ was taken from the fit.

III. GENERALIZATION OF FISHER'S RENORMALIZATION

As mentioned earlier, constrained critical phenomena can be successfully explained by the Fisher renormalization mechanism [23–27]. The basic idea of this mechanism is straight-forward and fundamental. It is based on the thermodynamic relation that, in the language of the BC model, the vacancy density ρ_v and the chemical potential D are conjugate parameters. Let f be the reduced free energy of the unconstrained critical model as a function of K and D. The constraint equation is then expressed as $\rho_v = -\partial f / \partial D = \text{const}$. This yields the path of the constrained system in the parameter space (K, D), which appears to be singular at the critical point. In this section, we follow a similar procedure and generalize the Fisher renormalization mechanism such that it can describe constrained tricritical phenomena. In particular, since the Monte Carlo simulations, which will be described in Sec. IV, have to take place at finite systems, we shall first focus on the finite-size scaling behavior of constrained tricritical systems.

As a first step, we express the finite-size scaling formula of the reduced free energy f of an unconstrained system [4] near the tricritical point as

$$f(t_1, t_2, L) = L^{-d} f_s(t_1 L^{y_{t1}}, t_2 L^{y_{t2}}) + f_a(t_1, t_2). \tag{24}$$

Here, L is the linear system size, and it can also be recognized as a scaling factor in the context of the renormalization group theory. The leading and subleading thermal scaling fields t_1 and t_2 represent the distance to the tricritical point at $t_1 = t_2 = 0$. The functions f_s and f_a are singular and analytical parts of the free energy f, respectively. We have neglected irrelevant scaling fields and also suppressed magnetic scaling fields in Eq. (24). For the BC model described by Eq. (1), the thermal fields t_1 and t_2 are analytic functions of K and D. Thus, differentiation of Eq. (24) with respect to D yields

$$-\langle \rho_v(t_1, t_2) \rangle = \frac{\partial f}{\partial D} = a_1 L^{y_{t1}-d} f_s^{(1,0)}(t_1 L^{y_{t1}}, t_2 L^{y_{t2}}) + a_2 L^{y_{t2}-d} f_s^{(0,1)} \times (t_1 L^{y_{t1}}, t_2 L^{y_{t2}}) + a_1 f_a^{(1,0)}(t_1, t_2) + a_2 f_a^{(0,1)}(t_1, t_2), \tag{25}$$

where $a_1 = \partial t_1 / \partial D$ and $a_2 = \partial t_2 / \partial D$ are constants. The superscripts (i, j) represent i differentiations with respect to t_1 and j differentiations with respect to t_2. Here, we mention that, for finite systems L, the conjugate quantity of D is the expectation value of the vacancy density $\langle \rho_v(t_1, t_2) \rangle$ instead of $\rho_v(t_1, t_2)$ itself. Under the constraint $\langle \rho_v(t_1, t_2) \rangle = \langle \rho_v(0, 0) \rangle$, Taylor expansion of Eq. (25) near the tricritical point leads to

$$0 = b_1 L^{2y_{t1}-d} t_1 + b_2 L^{y_{t1}+y_{t2}-d} t_2 + b_3 t_1 + b_4 t_2, \tag{26}$$

where b_1, b_2, b_3, and b_4 are constants, and *only* the leading terms are kept in the expansions of f_s and f_a. The constraint equation (26) describes the approach of the constrained BC model to the tricritical point in the parameter space (t_1, t_2). However, the analytic form of the path still depends on the relative values of y_{t1}, y_{t2}, and d, and so do the critical exponents describing the constrained critical singularities for $t_1, t_2 \to 0$. It follows from Eq. (26) that, near the tricritical point, the thermal fields t_1 and t_2 are related as follows.

(1) For $2y_{t1} - d > 0$ and $y_{t1} + y_{t2} - d > 0$, the first two terms in the right-hand side of Eq. (26) dominate as $L \to \infty$, so that one has $L^{y_{t1}} t_1 \propto L^{y_{t2}} t_2$, i.e., $t_2 \gg t_1$ and $K - K_{tc} \approx t_2$. Thus, the leading thermal exponent of the constrained system is equal to the subleading exponent y_{t2}.

(2) For $2y_{t1} - d > 0$ but $y_{t1} + y_{t2} - d < 0$, one has $L^{y_{t1}} t_1 \propto L^{d-y_{t1}} t_2$. The leading exponent is renormalized as $y_{t1} \to d - y_{t1}$. This case was already correctly included as one of the possible outcomes of Imry's renormalization calculations [28], as mentioned in Sec. I.

(3) For $2y_{t1} - d < 0$, i.e., the unconstrained specific heat does not diverge at tricriticality, t_1 is linearly related to t_2 as $t_1 \propto t_2$, and no exponent renormalization occurs.

In short, for a system with a divergent specific heat at tricriticality, critical exponents are renormalized under the constraint; otherwise, no renormalization occurs. However, since tricritical systems have two relevant thermal fields t_1 and t_2, the tricritical renormalizations can appear in different ways, depending on whether or not $y_{t1} + y_{t2} > d$.

Then the expression of the reduced free energy f' of the constrained tricritical BC model can be obtained by substitution of the above renormalization in Eq. (24), which yields

$$f'(t_1, t_2, L) = L^{-d} f'_s(t_1 L^{y'_{t1}}, t_2 L^{y_{t2}}, 1) + f'_a(t_1, t_2), \tag{27}$$

where y'_{t1} is equal to y_{t2}, $d - y_{t1}$, and y_{t1} for $y_{t1} + y_{t2} > d$, $y_{t1} + y_{t2} < d$ but $2y_{t1} > d$, and $2y_{t1} < d$, respectively.

Next, we consider the effect of the constraint in an infinite system. We interpret the parameter L in Eq. (24) as a rescaling factor that can be arbitrarily chosen. Thus, we may set the rescaling factor $L = t_2^{-1/y_{t2}}$ for case 1 and $L = t_2^{-1/(d-y_{t1})}$ for case 2, so that the thermal fields t_1 and t_2 are related as $t_1 \propto t_2^{y_{t2}/y_{t1}}$ and $t_1 \propto t_2^{(d-y_{t1})/y_{t1}}$, respectively. Substitution of these relation in Eq. (27) yields the constrained reduced free energy f' of an infinite system as

$$f'(t_1, t_2) \propto t_1^{2-\alpha'} \Psi(t_2 / t_1^{\phi}). \tag{28}$$

Here, the critical index is given by $\alpha' = 2 - d / y'_{t1}$ and the crossover exponent by $\phi = y_{t2} / y'_{t1}$, with y'_{t1} given earlier, and Ψ represents an analytical function. For the case $y'_{t1} = d - y_{t1}$, one has $\alpha' = -\alpha / (1 - \alpha)$, in agreement with Eq. (2).

During the derivation of these scaling equations, we have used Taylor expansions, for instance, of Eq. (25), and kept only the leading terms. Therefore, in addition to those from irrelevant thermal fields, we expect that new corrections are induced by the constraint.

Constrained tricritical behavior in three dimensions

As generally expected at the borderline dimensionality for mean-field-like behavior, logarithmic corrections to scaling occur in tricritical BC systems (1) in three dimensions. This has already been obtained in renormalization calculations of the Landau-Ginzburg-Wilson Hamiltonian. Near the tricritical point, the reduced free energy of the 3D BC model reads [4]

$$f(t_1,t_2,h_1,h_2,v,L) = L^{-3} f_s(t_1 L^2, t_2 L L_0^{-2/5}, h_1 L^{5/2}, h_2 L^{3/2} L_0^{-1/10}, v L_0^{-1}) + f_a(t_1,t_2), \tag{29}$$

where the parameter v, also an analytical function of K and D, describes the leading irrelevant thermal field. For completeness, we have also included the leading and subleading magnetic fields h_1 and h_2. The amplitude $L_0 = 1 + 25v \ln L$ accounts for the aforementioned logarithmic corrections. Equation (29) indicates that these corrections occur not only in the irrelevant field v but also in the subleading fields t_2 and h_2.

It follows from Eq. (29) that the unconstrained specific heat C in systems (1) is divergent ($2y_{t1} - 3 > 0$) at tricriticality, and thus the critical exponents are renormalized under the constraint. However, the 3D tricritical BC model (1) is a marginal case in the sense the critical exponents $y_{t1} + y_{t2} - 3 = 0$, so that it is not immediately obvious how the renormalization occurs. Taking into account $L_0^{-2/5}$ in Eq. (29) for the subleading field t_2, we conclude that in constrained systems the leading thermal exponent is renormalized as $y'_{t1} = 3 - y_{t1} = 1$.

IV. MONTE CARLO SIMULATIONS

A. Unconstrained BC models

The tricritical BC model (1) has been investigated on several three-dimensional lattices, and various techniques have been developed, including the self-consistent Ornstein-Zernike approximation [37] and Monte Carlo simulations [36,38].

In comparison with the well-known Swendsen-Wang [39] and Wolff [32] algorithms for the spin-$\frac{1}{2}$ Ising model, no cluster algorithm has so far been developed to efficiently flip between Ising spins and vacancies near the tricritical point. Thus, Monte Carlo simulations of the unconstrained tricritical BC model (1) suffer from critical slowing down. Using a combination of the Metropolis, Wolff, and aforementioned geometric cluster [29–31] steps, we simulated the BC model (1) on the simple-cubic lattice with periodic boundary conditions. The fluctuations between vacancies and Ising spins are realized by the standard Metropolis method; the Wolff algorithm flips between +1 and −1 Ising spins; and the geometric steps move groups of spins and vacancies over the lattice. In this way, critical slowing down is significantly suppressed. Making use of the exact values of Q_m and Q_v, as calculated in Sec. II, we located [36] the tricritical point as $K_t = 0.7133(1)$ and $D_t = 2.0313(4)$; the expectation value of the tricritical vacancy density is $\rho_{vt} = 0.6485(2)$, rather close to the mean-field value $2/3$. Consistency between these results and existing determinations [37,38], $K_t = 0.706(3)$, $D_t = 2.01(1)$, and $\rho_{vt} = 0.655(6)$, exists within a margin of about twice the quoted errors. Here, we have applied other techniques, including a simultaneous analysis of various quantities for different systems such that parameters in common appear only once [16]; the details of these numerical analyses will be presented elsewhere [36].

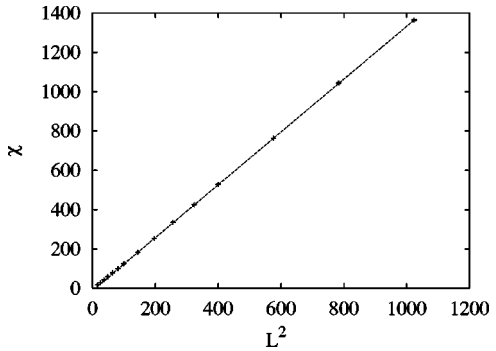

FIG. 5. The unconstrained magnetic susceptibility χ of the 3D BC model at tricriticality, shown vs $L^{2y_{h1}-3}$, with $y_{h1} = 5/2$.

For a comparison of constrained tricritical behavior, we simulated the constrained BC model at the tricritical point (K_t, D_t), as determined earlier, with system sizes $6 \leqslant L \leqslant 32$. We sampled the magnetic susceptibility χ, the energy density $\langle e \rangle$, the specific heat C, and the Binder ratios, etc., respectively. Here, the energy density $\langle e \rangle$ was defined as nearest-neighbor correlations, and the specific heat C reads

$$C = L^3 K^2 (\langle e^2 \rangle - \langle e \rangle^2), \tag{30}$$

representing the strength of critical fluctuations of $\langle e \rangle$. At tricriticality, the scaling behavior of these quantities can be derived from Eq. (29) as

$$\chi = x_0 \propto L^{2y_{h1}-3} = L^2, \ \langle e \rangle - e_0 \propto L^{y_{t1}-3} = L^{-1}, \ \text{and } C - c_0 \propto L^{2y_{t1}-3} = L, \tag{31}$$

where the terms x_0, e_0, and c_0 arise from the analytical part of the free energy. The Monte Carlo data for χ, $\langle e \rangle$, and C are shown in Figs. 5, 6, and 7, respectively. The approximate linearity for large L in these figures confirms the tricritical finite-size scaling behavior described by Eq. (31).

Apart from the conventional specific heat C, we also sampled a related quantity C_s on the basis of the Fourier components of $e(x,y,z)$ for systems of size L:

$$e_{k_x,k_y,k_z} = \frac{1}{L^3} \int_0^L dx\, dy\, dz\, e(x,y,z) \exp[2\pi \mathrm{i}(x k_x + y k_y + z k_z)/L]. \tag{32}$$

Obviously, $e_{0,0,0}$ is just the global energy density e; and quantities e_{k_x,k_y,k_z} for $k_x \neq 0$, $k_y \neq 0$, or $k_z \neq 0$ represent spatial

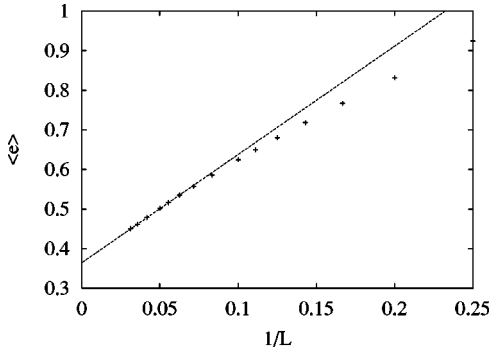

FIG. 6. The unconstrained energy density $\langle e \rangle$ of the 3D BC model at tricriticality, vs $L^{y_{t1}-3}$, with $y_{t1}=2$.

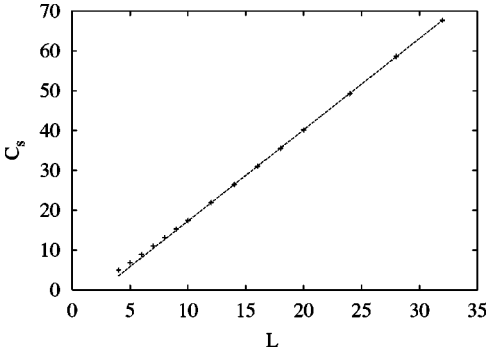

FIG. 8. The unconstrained structure factor of the specific heat C_s of the 3D BC model at tricriticality, vs $L^{2y_{t1}-3}$, with $y_{t1}=2$.

inhomogeneities of $e(x,y,z)$. Then, the quantity C_s can be defined in terms of e_{k_x,k_y,k_z} for the smallest wave numbers as

$$C_s = L^3 K^2 \langle e_{-1,0,0} e_{1,0,0} + e_{0,-1,0} e_{0,1,0} + e_{0,0,-1} e_{0,0,1} \rangle. \quad (33)$$

The physical meaning of C_s can be gleaned in comparison with the conventional specific heat C. First, as indicated by Eqs. (30) and (33), both quantities represent fluctuation strengths of e_{k_x,k_y,k_z}, with $k_x=k_y=k_z=0$ for C and $|k_x|+|k_y|+|k_z|=1$ for C_s. Second, both C and C_s can be expressed in terms of a sum of energy-energy correlation functions. Thus, we expect that C_s behaves as a specific-heat-like quantity, and we refer to it as the structure factor of the specific heat C. Then, the tricritical scaling behavior of C_s is also governed by Eq. (31), and this is confirmed by Fig. 8.

B. Constrained BC models

For the three-dimensional BC model (1) with a conserved number of vacancies, we used a combination of the Wolff and geometric cluster steps only. The chemical potential D in Eq. (1) becomes implicit and does not play a role in constrained Monte Carlo simulations. One particular feature is that these simulations *hardly* suffer from critical slowing down even near the tricritical point. This may be attributed to the fact that the constrained specific heat C does not diverge at tricriticality, as discussed later. Therefore, we extensively simulated systems in the range $6 \leqslant L \leqslant 128$. The coupling constant K and the vacancy density ρ_v were set at $K_{tc}=0.7133(1)$ and $\rho_{tc}=0.6485(2)$ [36], respectively. For a finite system, however, the number of vacancies $N_{vt}=L^3\rho_{tc}$ is not an integer, so that the actual simulations took place at $[N_{vt}]$ and $[N_{vt}]+1$, where the brackets [] denote the integer part. The value of a sampled quantity at N_{vt} was obtained by a linear interpolation between $[N_{vt}]$ and $[N_{vt}]+1$.

The Monte Carlo data for χ, $\langle e \rangle$, and C are shown in Figs. 9, 10, and 11, respectively. As illustrated by Figs. 5 and 9, the magnetic exponent describing the divergence of the susceptibility χ, i.e., y_{h1}, remains unchanged under the constraint, which indicates that the constraint on vacancies does not qualitatively influence magnetic quantities. However, the critical behavior of energylike quantities is significantly modified. In particular, the tricritical specific heat C is strongly suppressed so that it only takes a finite value as $L \to \infty$. This constrained phenomenon is in agreement with the generalized Fisher renormalization mechanism presented in Sec. III. Further, from Eqs. (27) and (29), the quantitative finite-size behavior of $\langle e \rangle$ and C at tricriticality is described by

$$\langle e \rangle - e_0 \propto L^{y'_{t1}-3} = L^{-2} \text{ and } C - c_0 \propto L^{2y'_{t1}-3} = L^{-1}, \quad (34)$$

where $y'_{t1}=3-y_{t1}=1$, as mentioned earlier. These theoretical predictions, i.e., Eq. (34), are reflected by the approximate linearity displayed by the data in Figs. 9 and 10. We fitted the data for $\langle e \rangle$ and C by

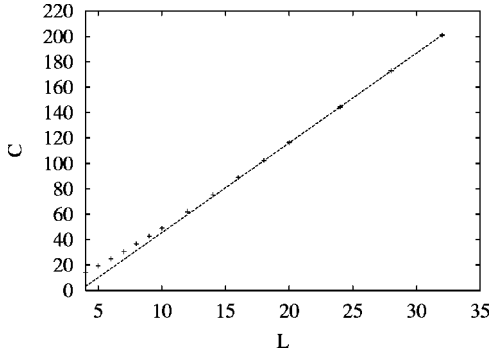

FIG. 7. The unconstrained specific heat C of the 3D BC model at tricriticality, vs $L^{2y_{t1}-3}$, with $y_{t1}=2$.

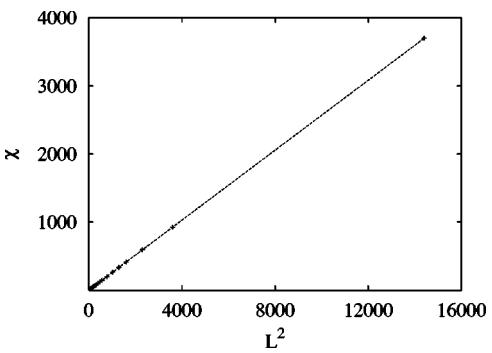

FIG. 9. The constrained magnetic susceptibility χ of the 3D BC model at tricriticality, vs $L^{2y_{h1}-3}$, with $y_{h1}=5/2$.

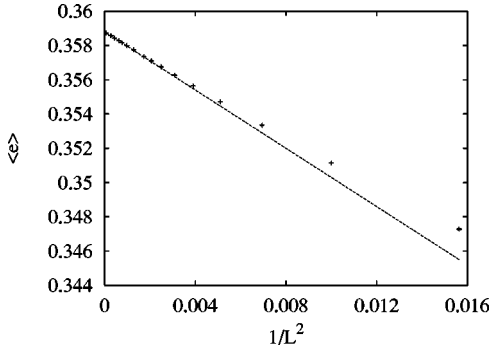

FIG. 10. The constrained energy density $\langle e \rangle$ of the 3D BC model at tricriticality, vs L^{-2}.

$$\langle e \rangle = e_0 + e_1 L^{y'_{t1}-3}(1 + b_1/\ln L + b_2/L + b_3/L^2) \qquad (35)$$

and

$$C = c_0 + c_1 L^{y'_{t1}-3}(1 + d_1/\ln L + d_2/L + d_3/L^2), \qquad (36)$$

respectively. The logarithmic corrections from the irrelevant fields are described by the terms with amplitudes b_1 and d_1. The fits of $\langle e \rangle$ and C yield that $y'_{t1}=0.99(2)$ and 1.02(2), respectively, with error margins of two standard deviations. This is consistent with the expectation $y'_{t1}=3-y_{t1}=1$. We mention that Eqs. (35) and (36) are in fact neither complete nor "correct" in describing the scaling behavior of $\langle e \rangle$ and C. First, one has not taken into account the second relevant thermal fields t_2, which can in principle introduce terms with $L_0^{-2/5}$ in the parentheses of Eqs. (35) and (36). Second, the logarithmic corrections should be described by terms with $1/L_0$ instead of $1/\ln L$. However, as indicated by the fits of $\langle e \rangle$ and C, this "bias" does not significantly affect the results of y'_{t1} due to the following reasons. The replacement of $1/\ln L$ by $(\ln L)^{-2/5}$ does not significantly change the result for y'_{t1}. Even neglecting the $1/\ln L$ term does not produce a large change. It appears that logarithmic corrections are not very serious in constrained tricritical systems. This is also illustrated by the clean intersection of the Q_m data for $K=K_t=0.7133(1)$ and $0.645 \leqslant \rho_v \leqslant 0.651$, partly shown in Fig. 12. The data for Q_m in the range $6 \leqslant L \leqslant 128$ were fitted by

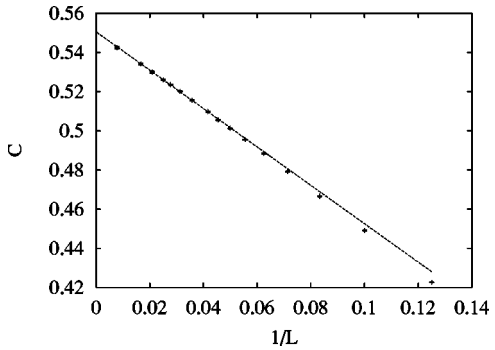

FIG. 11. The constrained specific heat C of the 3D BC model at tricriticality, vs L^{-1}.

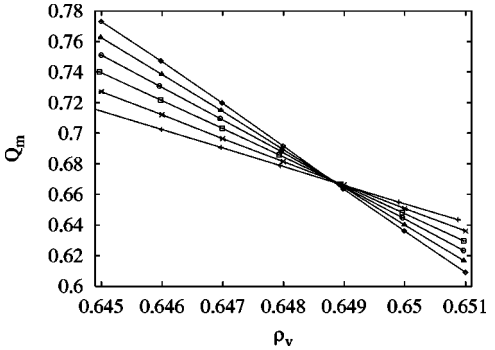

FIG. 12. The constrained Binder ratio Q_m of the 3D BC model for $K=0.7133(2)$, vs the vacancy density ρ_v. The data points are $L=16(+), 20\times$, 24 (□), 28 (◯), 32 (△), and 36 (◇)

$$Q_m(K,L) = Q_{mt} + \sum_{k=1}^{4} (\rho_v - \rho_{vt})^k L^{ky'_{t1}} + b_1/\ln L + b_2/L + b_3/L^2 + c(\rho_v - \rho_{vt})L^{y'_{t1}}/L, \qquad (37)$$

where ρ_{vt} is the tricritical vacancy density. The renormalized thermal exponent was taken as $y'_{t1}=1$, and we obtain $b_1=0.066(5)$ and $Q_{mt}=0.687(6)$, with two standard deviations again. The value of Q_{mc} is in agreement neither with $Q_t=1/2$ for unconstrained systems nor with the mean-field *critical* Ising value $Q_c=0.4567\ldots$.

The influence of the annealed constraint on tricritical spatial fluctuations can be reflected by the constrained Monte Carlo data for C_s at the tricritical point, as shown in Fig. 13. As in unconstrained systems, C_s diverges as $C_s \propto L$ as $L \to \infty$, so that the leading thermal exponent y_{t1} still governs the scaling behavior of C_s. This is rather different from the constrained behavior of the conventional specific heat C, which is suppressed to be convergent at tricriticality. We fitted the data for C_s by

$$C_s = c_{s0} + c_{s1} L^{y_{t1}-3}(1 + d_{s1}/\ln L + d_{s2}/L + d_{s3}/L^2), \qquad (38)$$

which yields $y_{t1}=1.995(8)$, in fine agreement with the exact value $y_{t1}=2$. Therefore, one can conclude that the tricritical spatial fluctuations remain unchanged under the constraint.

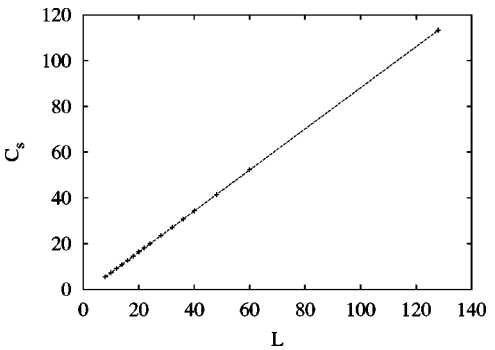

FIG. 13. The structure factor C_s of the constrained specific heat of the 3D BC model at tricriticality, vs L.

V. DISCUSSION

Due to the geometric cluster algorithm, a full-cluster simulation becomes possible for the tricritical BC model with a conserved number of vacancies. We have performed an extensive investigation of constrained tricritical behavior in three dimensions, and observe the following.

(1) The leading finite-size scaling behavior of magnetic quantities remains unchanged under the constraint. This is as expected: the vacancy density ρ_v is conjugate to the chemical potential D, which contributes only to the thermal fields t_1 and t_2.

(2) The critical behavior of energylike quantities is renormalized; particularly, the constrained specific heat C has only a finite cusp at tricriticality. The leading thermal exponent $y_{t1}=2$ is renormalized as $y'_{t1}=3-y_{t1}=1$, while the second one $y_{t2}=1$ remains unchanged under the constraint.

(3) The constrained magnetic Binder ratio at tricriticality is $Q_{mt}=0.687(6)$, apparently different from the unconstrained value $Q_{mt}=1/2$. This is understandable because the universal ratio Q_m still depends on boundary conditions, and the aspect ratios, etc., which influence magnetic correlation functions. The constraint also belongs to this category.

(4) Structure factors such as C_s, accounting for spatial inhomogeneities of conventional quantities, display the same scaling behavior as in unconstrained systems. This indicates that the divergence of the spatial correlation length, one essential characterization of critical phenomena, remains unchanged under the constraint at least to a scale that is small in comparison with system sizes. In this sense, one can conclude that the annealed constraint does not modify the universality class of a tricritical system.

As discussed in Sec. II, the constrained version of the mean-field tricritical BC model displays a behavior which is mean-field *critical* Ising-like. Apparently, this is different from the three-dimensional constrained tricritical behavior summarized above. This indicates that the mean-field theory is not complete in describing universal critical phenomena even at the upper critical dimensionality. For an unconstrained mean-field BC model, the vacancy fluctuations are coupled to the Ising fluctuations. Then, the stability criterion of the coupled fluctuations, depending on the value of K and D, yields distinct types of phase transitions: a line of critical Ising points, a tricritical point, and a first-order transition line. However, in constrained mean-field systems, the fluctuations of vacancies are suppressed. Therefore, the presence of vacancies *only* serves to reduce the number of Ising spins, leading to a smaller effective interaction. As a consequence, the whole line of phase transitions in the space (K,D), including the tricritical point and the first-order transition, reduces to meanfield *critical* Ising-like under the constraint. Since this does not agree with the constrained behavior of the investigated short-range model, we arrive at the somewhat surprising result that mean-field theory does not describe the universal properties of the constrained tricritical model at its upper critical dimensionality.

On the basis of the generalized Fisher renormalization mechanism, as outlined in Sec. III, we finite-size analyzed several tricritical quantities of the constrained BC model in three dimensions. The agreement between the theoretical predictions and the Monte Carlo results is quite satisfactory. We emphasize that, although the present annealed constraint leads to a change of the critical exponents, it does not modify the universality class. In fact, the derivations in Sec. III make essential use of the universal renormalization exponents.

The Fisher renormalization mechanism is rather straightforward and fundamental. Nevertheless, Imry's renormalization calculations [28] also give a correct prediction of the critical index α for tricritical $O(n)$ systems $(n \geqslant 1)$ in three dimensions. However, we mention that the calculations in Ref. [28] did not take into account the effect of the subleading thermal field y_{t2}. It is then justified to ask the question how to include y_{t2} in these calculations.

A final remark follows. In a finite system, the vacancy density ρ_v need not be equal to its expectation value $\langle \rho_v \rangle$, although this difference vanishes as $L \to \infty$. In the generalized Fisher mechanism for constrained tricritical behavior, it is only required that $\langle \rho_v(t_1,t_2) \rangle$ is equal to $\langle \rho_v(0,0) \rangle$. However, the Monte Carlo simulations take place with $\rho_v = \rho_{vt}$, i.e., no fluctuation of ρ_v is allowed. In this sense, the constraint in our numerical studies is "stronger" than the one in the generalized Fisher renormalization, although our present numerical results do not reveal the consequences of this fact.

ACKNOWLEDGMENTS

The authors are indebted to Professor M. E. Fisher, Professor Y. Imry, and Professor J. M. J. van Leeuwen for valuable discussions and comments, and to Dr. J. R. Heringa for his contribution to the development of the geometric cluster algorithm used in this work. This research is supported by the Dutch FOM foundation ("Stichting voor Fundamenteel Onderzoek der Materie") which is financially supported by the NWO ("Nederlandse Organisatie voor Wetenschappelijk Onderzoek").

[1] M. Blume, Phys. Rev. **141**, 517 (1966).
[2] H. W. Capel Physica (Amsterdam) **32**, 966 (1966); Phys. Lett. **23**, 327 (1966).
[3] L. Onsager, Phys. Rev. **65**, 117 (1944).
[4] For a review, see, e.g., I. D. Lawrie and S. Sarbach, in *Phase Transitions and Critical Phenomena*, edited by C. Domb and J. L. Lebowitz (Academic Press, London, 1984), Vol. 9, p. 1.
[5] B. M. McCoy and T. T. Wu, *The Two-Dimensional Ising Model* (Harvard University Press, Cambridge, MA, 1968).
[6] R. J. Baxter, J. Phys. A **13**, L61 (1980); J. Stat. Phys. **26**, 427 (1981).
[7] D. A Huse, Phys. Rev. Lett. **49**, 1121 (1982); R. J. Baxter and P. A. Pearce, J. Phys. A **16**, 2239 (1983).
[8] B. Nienhuis, A. N. Berker, E. K. Riedel, and M. Schick, Phys.

Rev. Lett. **43**, 737 (1979).
[9] B. Nienhuis, in *Phase Transitions and Critical Phenomena*, edited by C. Domb and J. L. Lebowitz (Academic Press, London, 1987), Vol. 11, p 1.
[10] A. A. Belavin, A. M. Polyakov, and A. B. Zamolodchikov, J. Stat. Phys. **34**, 763 (1984); D. Friedan, Z. Qiu, and S. Shenker, Phys. Rev. Lett. **52**, 1575 (1984).
[11] J. L. Cardy, in [9], p. 55.
[12] There is a typo in Ref. [9] about the second magnetic exponent; from private communications with B. Nienhuis, we have $y_{h2}=9/8$ for the tricritical BC model in two dimensions.
[13] For a review, see, e.g., K. Binder and E. Luijten, Phys. Rep. **344**, 179 (2001).
[14] M. Campostrini, A. Pelissetto, P. Rossi, and E. Vicari, Phys. Rev. E **65**, 066127 (2002).
[15] Y. Deng and H. W. J. Blöte, Phys. Rev. Lett. **88**, 190602 (2002).
[16] Y. Deng and H. W. J. Blöte, Phys. Rev. E **68**, 036125 (2003).
[17] For an introduction, see, e.g., S. K. Ma, *Modern Theory of Critical Phenomena* (Addison-Wesley, Redwood City, CA, 1976).
[18] Y. Achiam and Y. Imry, J. Phys. C **10**, 39 (1977).
[19] R. B. Stinchcombe, in *Phase Transitions and Critical Phenomena*, edited by C. Domb and J. L. Lebowitz (Academic Press, London, 1984), Vol. 7, p. 152.
[20] I. Syozi, Prog. Theor. Phys. **34**, 189 (1965); I. Syozi and S. Miyazima, *ibid.* **36**, 1083 (1966).
[21] D. C. Rapaport, J. Phys. C **5**, 1830 (1977); **5**, 2813 (1977).
[22] J. W. Essam and H. Garelick, Proc. Phys. Soc. London **92**, 136 (1967).
[23] M. E. Fisher, Phys. Rev. **176**, 257 (1968).
[24] Y. N. Skryabin and A. V. Shchanov, Phys. Lett. A **234**, 147 (1997).
[25] M. Krech, e-print cond-mat/9903288.
[26] I. M. Mryglod and R. Folk, Physica A **294**, 351 (2000).
[27] I. M. Mryglod, I. P. Omelyan, and R. Folk, Phys. Rev. Lett. **86**, 3156 (2001).
[28] Y. Imry, Phys. Rev. Lett. **33**, 1304 (1974); J. Rudnick, D. J. Bergman, and Y. Imry, Phys. Lett. A **46**, 448 (1974); Y. Achiam and Y. Imry, Phys. Rev. B **12**, 2768 (1975).
[29] J. R. Heringa and H. W. J. Blöte, Physica A **232**, 369 (1996).
[30] H. W. J. Blöte, E. Luijten, and J. R. Heringa, J. Phys. A **28**, 6289 (1995).
[31] J. R. Heringa and H. W. J. Blöte, Phys. Rev. E **57**, 4976 (1998).
[32] U. Wolff, Phys. Rev. Lett. **62**, 361 (1989).
[33] E. Luijten and H. W. J. Blöte, Int. J. Mod. Phys. C **6**, 359 (1995).
[34] E. Luijten, *Interaction Range, Universality and the Upper Critical Dimension* (Delft University Press, Delft, 1997).
[35] K. Binder, Z. Phys. B: Condens. Matter **43**, 119 (1981).
[36] Y. Deng and H. W. J. Blöte (unpublished).
[37] S. Grollau, E. Kierlik, M. L. Rosinberg, and G. Tarjus, Phys. Rev. E **63**, 041111 (2001).
[38] M. Deserno, Phys. Rev. E **56**, 5204 (1997).
[39] R. H. Swendsen and J. S. Wang, Phys. Rev. Lett. **58**, 86 (1987).